Macromolecules

pubs.acs.org/Macromolecules Article

Discrete Side Chains for Direct Tuning Properties of Grafted Polymers

Yiqing Wang, Xiao Tan, Yuhao Zhang, David J. T. Hill, Afang Zhang, Dehui Kong, Craig J. Hawker, Andrew K. Whittaker,* and Cheng Zhang*

Cite This: *Macromolecules* 2024, 57, 11753−11762 Read Online

ACCESS | Metrics & More | Article Recommendations | Supporting Information

ABSTRACT: Synthetic grafted polymers featuring a backbone main chain and functional oligomeric side chains have been widely used in a variety of high-value applications. However, dispersity in side-chain length limits the full understanding of their structure−property relationships. Herein, we report an efficient strategy to access grafted polymers with precisely controlled side-chain structure. Automated chromatography is utilized to separate a range of commercially available, disperse (meth)acrylate ethylene glycol and propylene glycol macromonomers into discrete, well-defined species. The separated macromonomers were subsequently employed to prepare grafted polymers having a discrete side-chain length and structure through controlled radical polymerization. By studying these well-defined materials, our results highlighted the influence of side-chain length and dispersity on various physical properties, including glass transition temperature and thermoresponsive behavior. Additionally, we observed that the length of the side chain has a more significant influence than the degree of polymerization of the main chain in determining these properties. This study confirms the versatility of automated chromatography for fractionating commercially available macromonomers and oligomeric cross-linkers into discrete species. From these building blocks, libraries of well-defined graft architectures and network grafted polymers can be prepared, which allows for a comprehensive understanding of structure−property relationships.

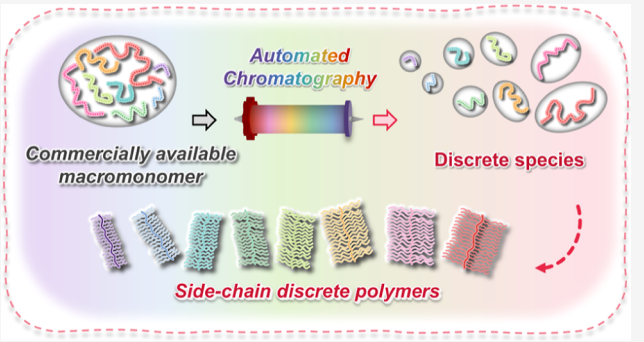

INTRODUCTION

Biological macromolecules, such as DNA and proteins, possess precisely defined structures and compositions that are crucial for their function. However, strategies to prepare monodisperse synthetic polymers using one-step direct polymerization techniques do not exist due to the inherent statistical nature of polymer growth processes. In contrast, the synthesis of discrete materials using multistep strategies has been widely reported and involves successive steps of monomer coupling and protecting group removal, leading to accurate control over structure.[1−3] Unfortunately, the existing stepwise approaches to discrete oligomers ($Đ$ = 1.0) are impractical for large-scale synthesis due to their time-consuming and multistep procedures. Limitations on the structure of the repeat units that are compatible with this stepwise process have also been observed.

Controlled polymerization techniques, such as atom transfer radical polymerization and reversible addition−fragmentation chain transfer polymerization (RAFT), have been widely used in research laboratories to prepare so-called "precisely defined" polymers; however, dispersity in molecular weight and composition is still present. Recently, a versatile and scalable automated flash chromatography method for preparing discrete oligomers ($Đ$ = 1.0) has been reported by Hawker, Zhang, and co-workers.[4−10] By using a mixed solvent system, this method can successfully separate polydisperse polymers (e.g., poly(ethylene glycol) and ethyl acetate/THF eluent) into discrete species.[11] A key advantage of this approach is the ability to purify a wide range of commercially available oligomers and polymers, which allows access to molecular-defined libraries that can be directly compared to traditional disperse materials, enabling both fundamental studies and targeted technological applications. We should note that previous work in chromatographic fractionation mainly focused on the preparation of materials having controlled main-chain dispersity. In contrast, the impact of side-chain dispersity on the properties of grafted polymers has received less attention, even though the properties of grafted polymers can be significantly influenced by the length of side chains. For

Received: October 16, 2024
Revised: November 25, 2024
Accepted: November 28, 2024
Published: December 4, 2024

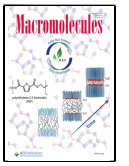

Scheme 1. Schematic Illustration of the Preparation of Grafted Polymer Materials with Dispersed and Discrete Side-Chain Lengths[a]

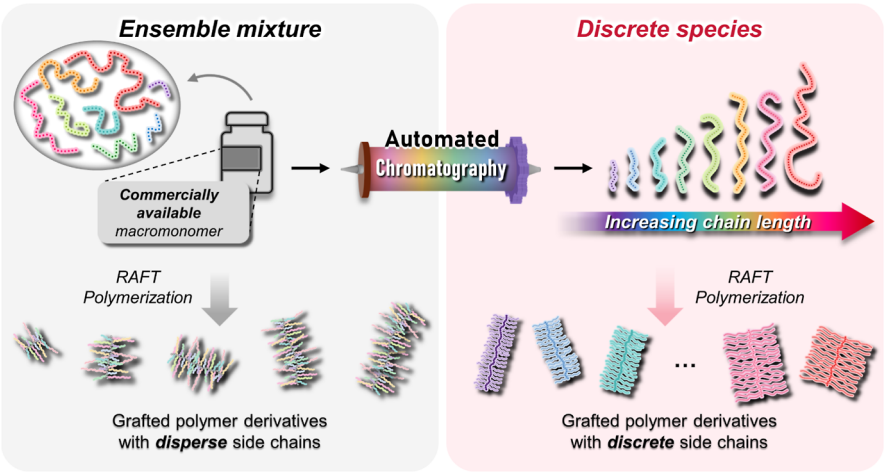

[a]Commercially available macromonomers were first fractionated using automated chromatography. Grafted polymer materials were then prepared by free radical polymerization techniques using either as-purchased parent disperse or fractionated discrete macromonomers.

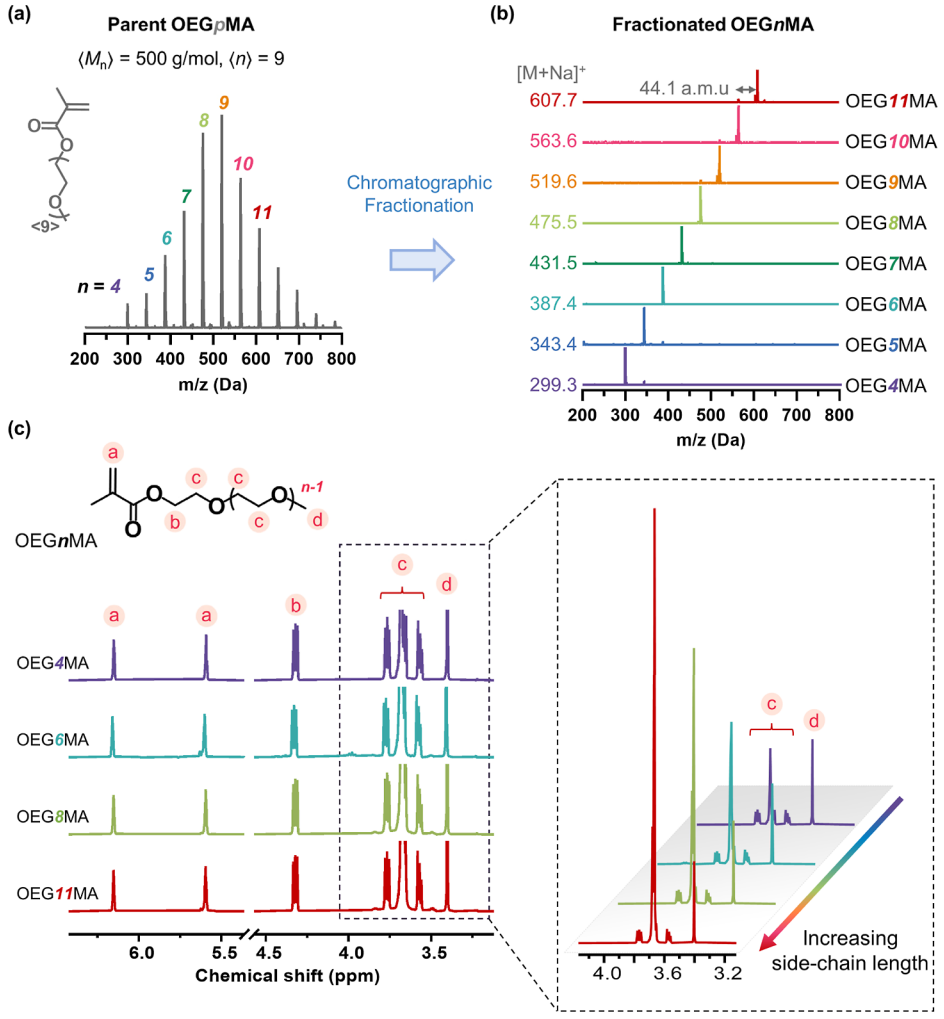

Figure 1. LC−MS spectra of (a) the parent OEG*p*MA and (b) the fractionated OEG*n*MA macromonomers. (c) Selected ^{1}H NMR spectra and chemical structures of fractionated OEG*n*MA macromonomers. Inset: zoom-in view of the region of EG repeating units. All spectra are normalized to the resonance belonging to the terminal methyl group (peak d, ∼3.4 ppm).

example, Benetti and co-workers demonstrated that polymer brush films with discrete oligo-oxazoline side chains exhibit distinct interfacial properties compared to those with heterogeneous structures.[12] Additionally, Lawrence and co-

https://doi.org/10.1021/acs.macromol.4c02533
Macromolecules 2024, 57, 11753−11762

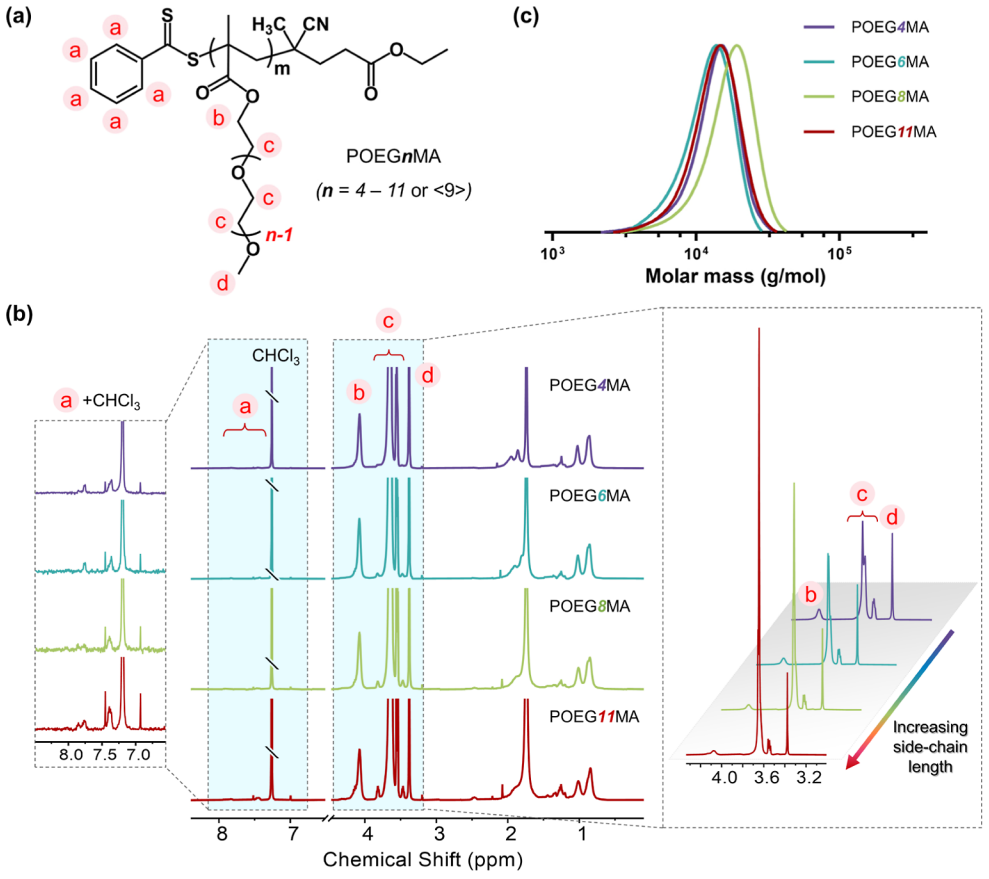

Figure 2. Characterization of disperse POEG*p*MA-grafted polymers. (a) Chemical structure, (b) ^{1}H NMR spectra, and (c) SEC spectra, indicating the successful synthesis of POEGMA-grafted polymers. Left inset: zoom-in spectra of the aromatic proton (backbone) region. Right inset: zoom-in spectra of methylene proton and methyl proton on the side chains. All spectra are normalized to the resonance for the terminal methyl protons (peak d, ∼3.4 ppm).

workers showed that precise control of side-chain length, rather than backbone length, allowed fine-tuning of the T_g in styrene-based bottlebrush polymers.[13] A key study by Lutz and co-workers reported that the lower critical solution temperature (LCST) of polymers prepared using 2-(2-methoxyethoxy)ethyl methacrylate (MEO_2MA, EG units = 2), tri(ethylene glycol) methyl ether methacrylate (EG units = 3), and disperse oligo(ethylene glycol) methyl ether methacrylates ($OEGMA_{300}$, average number of EG units = 4.5 or $OEGMA_{475}$, average number of EG units = 8.5) increases from 26 to 52 to 64 and 90 °C, respectively, as the side-chain length increases.[14] These unique thermoresponsive EG-based polymers with tunable side-chain structure and LCST properties have received significant attention from researchers for a number of high-value applications. However, unlike macromolecules produced by biological systems having a discrete chemical structure,[15−17] commercially available ethylene glycol (meth)acrylate macromonomers (e.g., $OEGMA_{300}$ and $OEGMA_{475}$) have molar mass dispersity within the EG side chains. The properties of grafted polymers prepared using macromonomer mixtures are therefore dictated by an ensemble mixture of polymers with different side chain and backbone lengths, each potentially with unique solubility and properties.[3,18,19]

In this study, we employ a combination of automated chromatographic fractionation with free radical polymerization to prepare a library of functional grafted polymer materials having discrete side-chain lengths (Scheme 1). Key to the success of this strategy is the use of disperse, commercially available parent macromonomers, such as oligo(ethylene glycol) methyl ether methacrylate (OEG*p*MA, $\langle M_n \rangle \approx 500$ g/mol, angle brackets $\langle \cdots \rangle$ are used to denote the average molecular weight), oligo(ethylene glycol) dimethacrylate (OEG*p*DMA, $\langle M_n \rangle \approx 550$ g/mol), oligo(propylene glycol) methacrylate (OPG*p*MA, $\langle M_n \rangle \approx 375$ g/mol), and oligo(ethylene glycol) methyl ether acrylate (OEG*p*A, $\langle M_n \rangle \approx 480$ g/mol). All four of these systems could be fractionated to produce a scalable library of discrete macromonomers with a discrete number of side chain repeating units and polymerizable (meth)acrylate chain end(s). Free radical polymerization techniques, such as RAFT, were subsequently conducted to prepare a series of grafted polymers with discrete side-chain lengths. The dependence of physical properties on side-chain dispersity was systematically investigated by using both the parent and fractionated polymers with disperse and discrete side-chain lengths. Our results highlight that side-chain dispersity has a significant impact on physical properties, such as glass transition temperature and thermoresponsive behavior in LCST. The length of the side chain plays a more pronounced role than the degree of polymerization (DP) of the main chain in determining these properties. The synthetic availability of a library of discrete macromonomers from commercially available starting materials, coupled with the control over the properties of grafted polymers, makes this an important class of well-defined macromolecular architecture for a range of fundamental studies and important applications.

https://doi.org/10.1021/acs.macromol.4c02533
Macromolecules 2024, 57, 11753−11762

Table 1. Properties of Fractionated Discrete OEG*n*MA Macromonomers and Their Corresponding Polymers, as Well as the Parent POEG*p*MA Polymers with Different DPs

polymers	$M_{n,macromonomer}$ (g/mol)[a]	DP[b]	$M_{n,NMR}$ (g/mol)[b]	$M_{n,GPC}$ (g/mol)[c]	$Đ$[c]	LCST (°C)[d]<	T_g (°C)[e]
POEG4MA	299.3	37	10,500	12,800	1.15	42	−53.4
POEG5MA	343.4	31	10,100	15,400	1.15	50	−56.9
POEG6MA	387.4	32	11,900	11,600	1.15	53	−58.9
POEG7MA	431.5	22	9200	6000	1.17	60	−60.9
POEG8MA	475.5	32	14,900	16,100	1.16	70	−62.2
POEG9MA	519.6	25	12,900	10,700	1.13	74	−62.9
POEG10MA	563.6	34	18,700	20,800	1.19	76	−63.3
POEG11MA	607.7	26	15,500	12,800	1.15	79	−63.9
POEG*p*MA-5	⟨500⟩	5	2800	7100	1.14	66	−61.0
POEG*p*MA-10	⟨500⟩	10	5300	9800	1.13	69	−61.2
POEG*p*MA-15	⟨500⟩	15	7800	11,900	1.10	73	−62.6
POEG*p*MA-25	⟨500⟩	25	12,800	17,800	1.11	71	−62.7
POEG*p*MA-35	⟨500⟩	35	17,800	21,400	1.14	69	−62.9
POEG*p*MA-45	⟨500⟩	45	22,800	27,300	1.18	68	−62.9
POEG*p*MA-55	⟨500⟩	55	27,800	30,000	1.16	67	−63.4

[a]The $M_{n,macromonomer}$ for the fractionated OEG*n*MA was measured by LC−MS, see Figure 1. The molecular weight is shown in the form of $[M + Na]^+$. [b]The DP and M_n, NMR of grafted polymers were calculated by considering the integrals of the peaks a and c, as shown in Figures 2 and S5. DP refers to the degree of polymerization of polymer backbone. [c]The M_n, SEC and $Đ$ were obtained by SEC in DMF. [d]LCST of grafted polymers was measured by UV−vis at 500 nm in 10× phosphate-buffered saline (PBS) buffer solution. [e]The T_gs was determined using DSC tested at 10 °C/min cooling/heating rate. T_g data presented in this table was collected from the heating scan of the second cycle.

RESULTS AND DISCUSSION

In order to demonstrate how properties of grafted polymers depend on side-chain dispersity, fractions of the parent disperse OEG*p*MA macromonomer were prepared and subsequently polymerized by RAFT polymerization. The commercially available parent OEG*p*MA macromonomer ($\langle M_n \rangle \approx 500$ g/mol, average number of EG unit ≈8−9) has dispersity in the number of ethylene glycol units as illustrated by liquid chromatography−mass spectrometry (LC−MS) analysis (Figure 1a). It should be noted that the parent OEG*p*MA macromonomer is a disperse mixture with the number of EG repeating units ranging from 4 to 14+ and molar mass from 299 to >750 g/mol. The dispersity, of the OEG*p*MA calculated from the LC−MS spectrum, and assuming quantitative relative intensities across this molecular weight range, is 1.03.

Automated chromatography was then employed to fractionate the parent OEG*p*MA (Figure S1a) using an optimized dichloromethane/tetrahydrofuran solvent gradient with standard columns (thin layer chromatography analysis for optimizing the solvent gradient is shown in Figure S1b, and the detailed gradient profile of the eluent is recorded in Table S1). A key advantage of this approach is scalability, which allows separations to be conducted on multigram scales. For example, from an 8.0 g commercial sample, a library of discrete OEG*n*MA macromonomers with precise side-chain lengths (*n* from 4 to 11) could be easily obtained in a two-stage procedure with total mass recovery being 80+% and the mass obtained for each discrete species ranging from 150 mg to 1.60 g. As shown in Figure 1b, each discrete sample is characterized by a single molecular ion, which correlates with the expected OEG*n*MA macromonomer structures being separated by 44.1 a.m.u., which corresponds to a single EG repeating unit. Figure S1c illustrates typical elution profiles obtained from the evaporative light-scattering detector (ELSD, BUCHI) with broad peaks corresponding to discrete OEG*n*MA macromonomers (*n* = 4 to 8) being observed. The scalability and preparative ease of this strategy highlight the power of combining readily available starting materials with automated chromatography and controlled polymerization procedures.

^{1}H NMR was used as a primary structural identification tool to confirm the successful fractionation and purity of the discrete OEG*p*MA libraries. The chemical structures of the fractionated OEG*n*MA macromonomers are shown in Figure 1c. All peaks could be successfully assigned, and intensities were normalized against the integration value for the unique terminal methyl group of each OEG side-chain. A linear increase in peak intensity of peak c (~3.6 ppm) can be observed with increasing side-chain length for the fractionated OEG*n*MA macromonomers (inset, Figure 1c), clearly illustrating the discrete nature of the library components. It should also be noted that the simple and mild nature of this purification technique allows for samples with reactive/polymerizable chain ends to be separated, with minimal to no side reactions being observed.

The RAFT agent ethyl 4-cyano-4-(thiobenzoylthio)-pentanoic acid (CPADB-ethyl CTA) was prepared (Figure S2) according to a literature method.[20] Grafted polymers were synthesized based on both the fractionated, discrete OEG*n*MA (POEG*n*MA) derivatives and the parent, disperse starting material OEG*p*MA (Figures 2 and S3). In this work, POEG*n*MA refers to polymers with well-defined side-chain lengths, where *n* denotes the number of repeat units in the side chains. The backbone DP for these polymers was maintained at approximately 30. In contrast, POEG*p*MA refers to the polymer prepared from the parent OEG*p*MA, which has a disperse side-chain length distribution and a broader range of backbone DP values, spanning from 5 to 55. Both sets of polymers were synthesized via RAFT polymerization using CPADB-ethyl CTA as the chain transfer agent. In situ NMR could be used to monitor the kinetics of RAFT polymerization, and as shown in Figure S3, the conversion at each predetermined time point is calculated by integration of the residual monomer peaks at ~6.5 ppm (peak a, 1H) and comparison to the newly formed broad polymer peaks at ~4.5 ppm (peak b, 2H).[21] As expected for a controlled RAFT

https://doi.org/10.1021/acs.macromol.4c02533
Macromolecules 2024, 57, 11753−11762

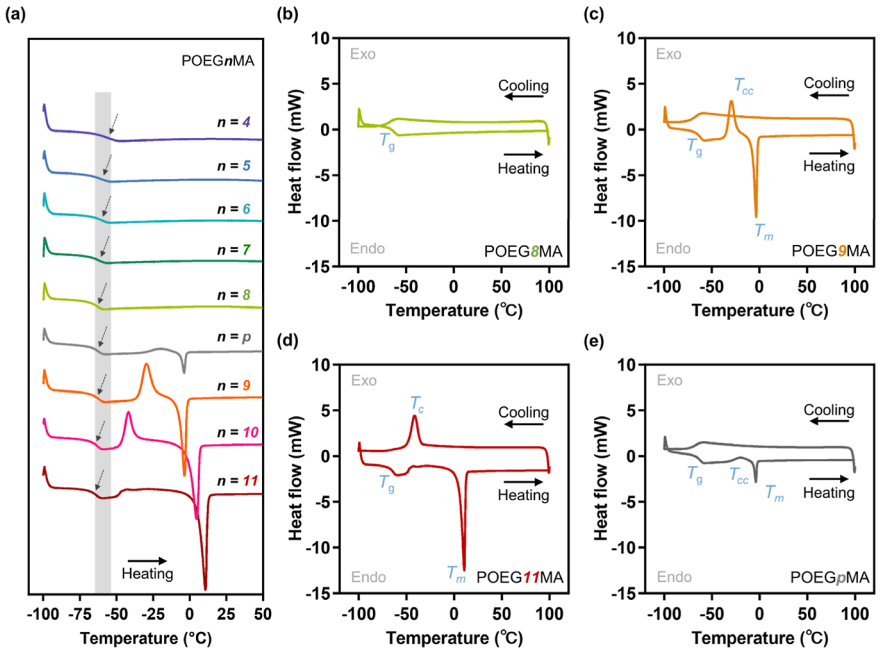

Figure 3. (a) DSC curves of POEG*p*MA and POEG*n*MA, T_g were highlighted by arrows. Individual DSC thermograms of grafted homopolymers (b) POEG8MA, (c) POEG9MA, (d) POEG11MA, and (e) POEG*p*MA (DP ∼ 35).

process, a linear increase of $\ln([M_0]/[M_t])$ versus reaction time was observed, indicating that the polymerizations follow pseudo-first-order kinetics without significant termination reactions (Figure S4). The ^{1}H NMR spectra and size exclusion chromatography (SEC) curves of the grafted polymers after purification are shown in Figures 2b,c and S5, confirming the successful synthesis of both POEG*p*MA and the corresponding library of POEG*n*MA derivatives with discrete side chains and well-defined backbone DPs. The detailed structural characteristics of the homopolymers are summarized in Table 1, with all discrete OEG*n*MA macromonomers, leading to controlled molecular weight products with narrow dispersity ($Đ$ < 1.19). These were purified using standard techniques and used directly for the following studies of thermal behavior.

A DSC study of the POEG*n*MAs and POEG*p*MAs reveals that changes in the glass transition temperature (T_g) are more pronounced with varying length of side chains compared to changes in the backbone length (i.e., DP). To be more specific, the phase transition for all POEG*p*MA materials occurs within the range of approximately −61.0 to −63.4 °C over a wide range of disperse DP values from 5 to 55. In contrast, the T_g of POEG*n*MAs exhibits a gradual decrease from −53.4 to −63.9 °C as the side-chain length increases from n = 4 to 11 (highlighted in the gray zone of Figure 3a), indicating the greater chain mobilities for side-chains with an increasing number of EG units. Compared to the backbone, changes in side-chain length have a greater impact on chain flexibility and free volume, resulting in a more pronounced effect on T_g.[13,22]

Crystallization was not observed for the POEG*n*MA-grafted polymers with EG units less than $n \leq 8$ due to the short side-chain length and limited segmental freedom that hinders the formation of an ordered arrangement (Figures 3b and S6a−d). As shown in Figures 3c and S6e, cold crystallization transitions (T_{cc}) were observed when the side-chain length increased to n = 9 and 10 for the discrete POEG9MA and POEG10MA systems, representing a unique crystallization phenomenon accompanying an exothermal anomaly when the polymer materials were heated within a temperature range below its melting point T_m.[23,24] The occurrence of cold crystallization mainly arises from a lack of sufficient time for crystallization during the cooling process. Instead, small crystals form at temperatures above T_g but below the melting temperature (T_m) during the subsequent heating sequence. When the side-chain length further increases to n = 11, the POEG11MA-grafted polymer exhibits a typical exothermic crystallization behavior during the cooling process (Figure 3d), indicating the polymer side chain has sufficient mobility and flexibility for rapid aligning and crystallizing.

In contrast, the POEG*p*MA polymers, spanning DPs from 5 to 55 and prepared using disperse parent macromonomer, did not display obvious crystallization (Figures 3e and S7). Instead, a small, broad peak occurring immediately before T_m during the heating run was identified as cold crystallization partially coupled with melting. The presence of dispersed side chains in the parent grafted polymers introduces heterogeneity that is detrimental to the formation of ordered arrangements. While the degree of crystallinity of the parent derivatives is low, the observed small endothermic T_m peak during the heating program reflects the melting of the parent polymer. Such dramatic differences in thermal properties observed between the parent and discrete libraries, coupled with the distinctive characteristics exhibited by each discrete derivative, highlight the importance of our approach to access well-defined grafted polymers.

The thermoresponsive properties of the POEGMA polymers were then investigated through turbidimetry measurements. The transmittance of the polymer solutions at 500 nm during heating and cooling at 1 °C/min (25 ↔ 90 °C) was monitored, and the LCST was defined as the temperature at which the light transmittance dropped to 50% during the heating run.[25] To adjust the LCST to a measurable range, a concentrated 10× PBS solution was employed.[26,27] It was found that the LCST of the discrete POEG*n*MA library increases in a well-defined trend with increasing numbers of

https://doi.org/10.1021/acs.macromol.4c02533
Macromolecules 2024, 57, 11753−11762

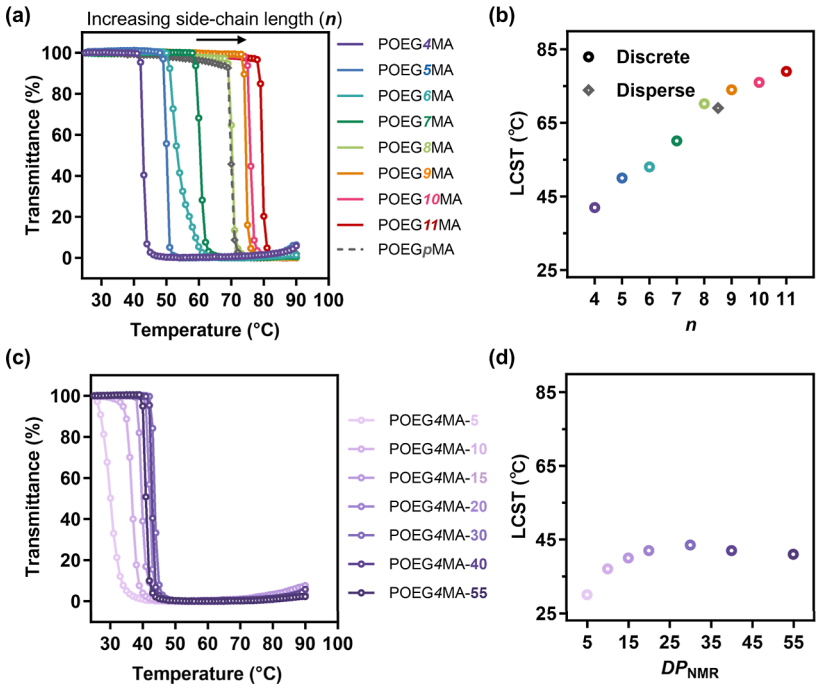

Figure 4. Volume phase transitions of polymer solutions. (a) Plots of transmittance as a function of temperature measured in 10× PBS solutions (2 mg/mL) of POEG*n*MA (solid lines) and POEG*p*MA (dashed lines). (b) Plots of LCSTs as a function of side-chain EG length of POEG*n*MA (n = 4 to 11). (c) Plots of transmittance as a function of temperature measured in 10× PBS solutions (2 mg/mL) of POEG4MA. (d) Plots of LCSTs as a function of DP (determined by ^{1}H NMR) of POEG4MA. Only the heating cycles were plotted in (a) and (c).

EG units in the side-chains of the polymers (i.e., LCST = 42, 50, 53, 60, 70, 74, 76, and 79 °C for n = 4 to 11, respectively, Figure 4a,b). The LCST depends on the balance of hydrophilic (OEG) segments and hydrophobic groups (i.e., polymer backbone), and as the length of the side chain increases, the graft polymer becomes more hydrophilic, resulting in an increase in LCST.[14] More specifically, the ether oxygen atoms of the hydrophilic OEGMA side chain form hydrogen bonds with water, while the hydrophobic methacrylate backbone reduces water solubility.[28] Such observations highlight the close relationship between side-chain length and thermoresponsive behavior and further highlight the importance of discrete well-defined libraries for examining structure/property relationships. It should be noted that the LCST behavior of POEG*p*MA results from contributions from the full ensemble of POEG*n*MA-grafted polymers, with the LCST of the disperse, parent POEG*p*MA system being close to the discrete POEG8MA derivative (69 vs 70 °C) since the length of the discrete side chain is close to the average chain length for the parent oligomer. Similar observations were reported by Lutz and co-workers, who demonstrated that adjusting the feed ratio of MEO2MA (EG = 2) and OEGMA475 (EG = 8/9) led to LCST values that are the weighted average of temperatures based on comonomer composition.[29]

We further investigated the potential influence of overall molecular weight (i.e., main-chain length) on the LCST. The LCST of the parent, disperse POEG*p*MA, exhibits an increase of 7 °C as the backbone DP increases from 5 to 15, corresponding to a molecular weight change from ∼2800 to ∼7800 g/mol (Figure S9a,b). Subsequently, a decrease in LCST from 73 to 67 °C was observed as the molecular weight of POEG*p*MA increased from ∼7800 to ∼30,000 g/mol (DP increases from 15 to 55). A similar observation was made when investigating the LCST dependence on the backbone DP for a library of POEG4MAs (i.e., DP = 5, 10, 15, 20, 30, 40, and 55, as shown in Table S2 and Figure S8), with a discrete side-chain length n = 4. The LCST increases as the DP of POEG4MAs rises until the molecular weight reaches ∼10,000 g/mol (DP ≈ 20), followed by a gradual decrease, similar to the above observation for the POEG*p*MA system. The shifts in LCST for different main-chain lengths in both POEG*p*MA (66 → 73 °C) and POEG4MA (30 → 43 °C) are relatively minor compared to the changes resulting from variations in side-chain length (POEG*n*MA, 42 → 79 °C, n = 4−11). The results presented in Figures 4 and S9 emphasize that the side-chain length exerts a much more pronounced effect on thermal properties than the length of the main chain.

The change in size for the assembled structures with temperature was also monitored by dynamic light scattering. A significant increase in hydrodynamic diameter (D_h) was observed, indicating a transition from unimers (i.e., single chain coils <10 nm) to large aggregates (∼1000 nm) upon reaching the LCST (Figure S10). These observations are consistent with turbidity measurements and further highlight the importance of side-chain length in determining the LCST.

As discussed previously, the transmittance of POEG*n*MA exhibits a sharp change when it is heated. This transition is due to a shift from a hydrated, expanded state to a collapsed state, resulting in a significant change in optical properties. The sudden transformation underscores the sensitivity of these graft polymers to temperature variations. However, broad heating−cooling hysteresis was observed in both POEG*p*MA and POEG*n*MA (Figures 5 and S11). This behavior arises from the slow relaxation and rehydration processes involved in the globule-to-coil transition on cooling as demonstrated by Lutz.[29] As expected, graft polymers with shorter EG side chains are overall more hydrophobic in nature and have a stronger tendency to phase separate from solution, i.e.,

https://doi.org/10.1021/acs.macromol.4c02533
Macromolecules 2024, 57, 11753−11762

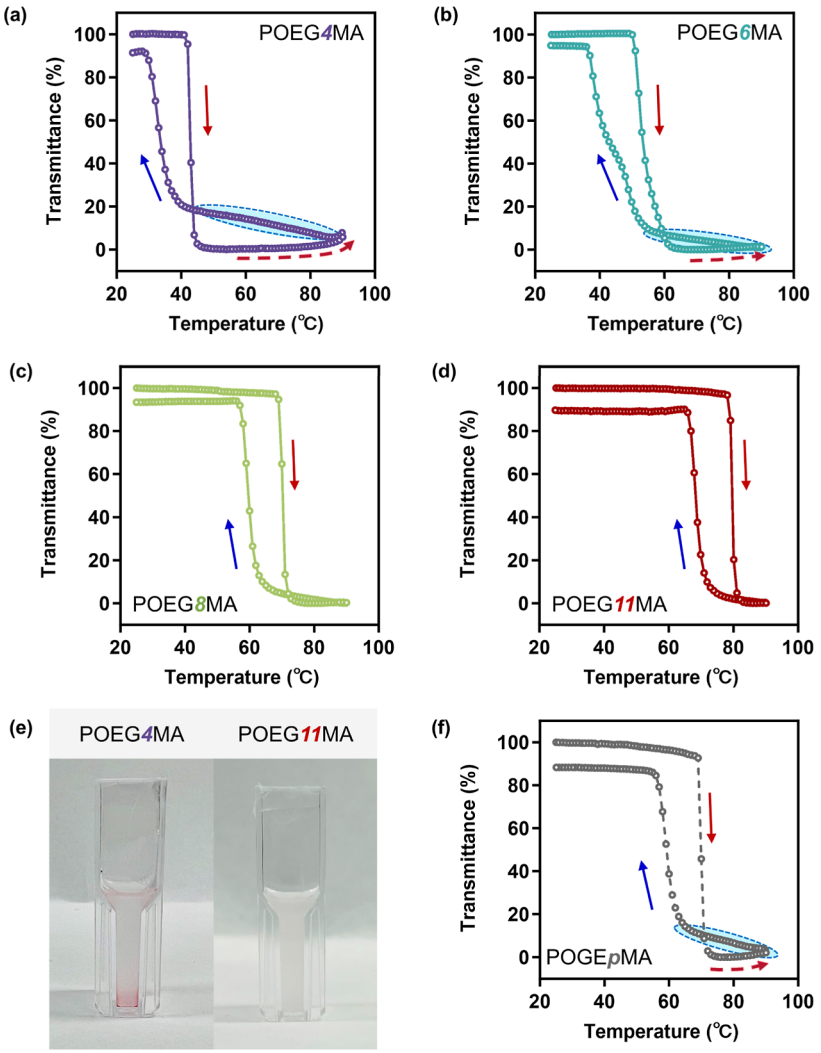

Figure 5. Plots of transmittance as a function of temperature measured by UV−vis: red and blue arrows represent heating and cooling cycles, respectively. (a−d,f) Measurements of samples POEG4MA, POEG6MA, POEG8MA, POEG11MA, and POEG*p*MA (*average n* = 9), respectively. (e) Photos of POEG4MA (left) and POEG11MA (right) polymers in 10× PBS solution at 90 °C after the heating process from 25 °C at 1 °C/min.

precipitate, during the heating process. In contrast, graft polymers with longer EG side chains are more hydrophilic. At side chain lengths of $n > 6$, these polymers form stable aggregates upon heating, which we describe as mesoglobules, referring to intermediate polymer aggregates that form above the phase transition, as opposed to full precipitation. POEG4MA, with the shortest, discrete side chains of the series, has a decrease in transmittance at 42 °C on heating (Figure 5a). When the POEG4MA solution is heated to 90 °C, a precipitate (color arising from the RAFT end group) forms at the bottom of the cuvette (Figure 5e). This results in a slight increase in transmittance on increasing temperature above the LCST for the polymers with the shortest side chains ($n = 4$ and 6), indicated by red dashed arrows in Figure 5a,b. On cooling, a pronounced hysteresis was observed due to the slower rehydration of the chain segments. It can also be seen that on cooling of the polymers with the shortest side chains, the transmittance on cooling was higher than observed during the heating cycle (highlighted with the blue circles in Figure 5a,b), and this is due to the partial rehydration of the precipitates. Graft polymers having longer side chains (e.g., POEG11MA, Figure 5d) are more hydrophilic and do not precipitate during the heating process but rather form mesoglobules (Figure 5e). For these systems, the transmittance at the beginning of the cooling process is similar to that at the end of the heating process. The polymers prepared by using the parent OEG*p*MA with an ensemble of side chain lengths show an averaged transmittance behavior, featuring a LCST similar to that of discrete POEG8MA with medium side chain lengths. Additionally, POEG*p*MA exhibit precipitation in the late heating and hysteresis during cooling, phenomena observed only in the discrete polymers with side chain lengths of $n < 6$, as illustrated in Figure 5f.

The above observations can be explained by the formation of "dense" or "loose" aggregates during the heating process for polymers with short and long side chains, respectively. The polymers with short side chains ($n < 7$) aggregate into compact "dense clusters" and partially precipitate out of the solution during the heating process. In contrast, polymers possessing medium-length and long side chains ($n \geq 7$) form "loose" aggregates, and the majority of these aggregates are dispersed in water in the form of mesoglobules. During cooling, the "loose" aggregates disperse to solvated individual coils as water becomes a good solvent, whereas the rehydration of the densely packed, precipitated aggregates is a slower process.

https://doi.org/10.1021/acs.macromol.4c02533
Macromolecules 2024, 57, 11753−11762

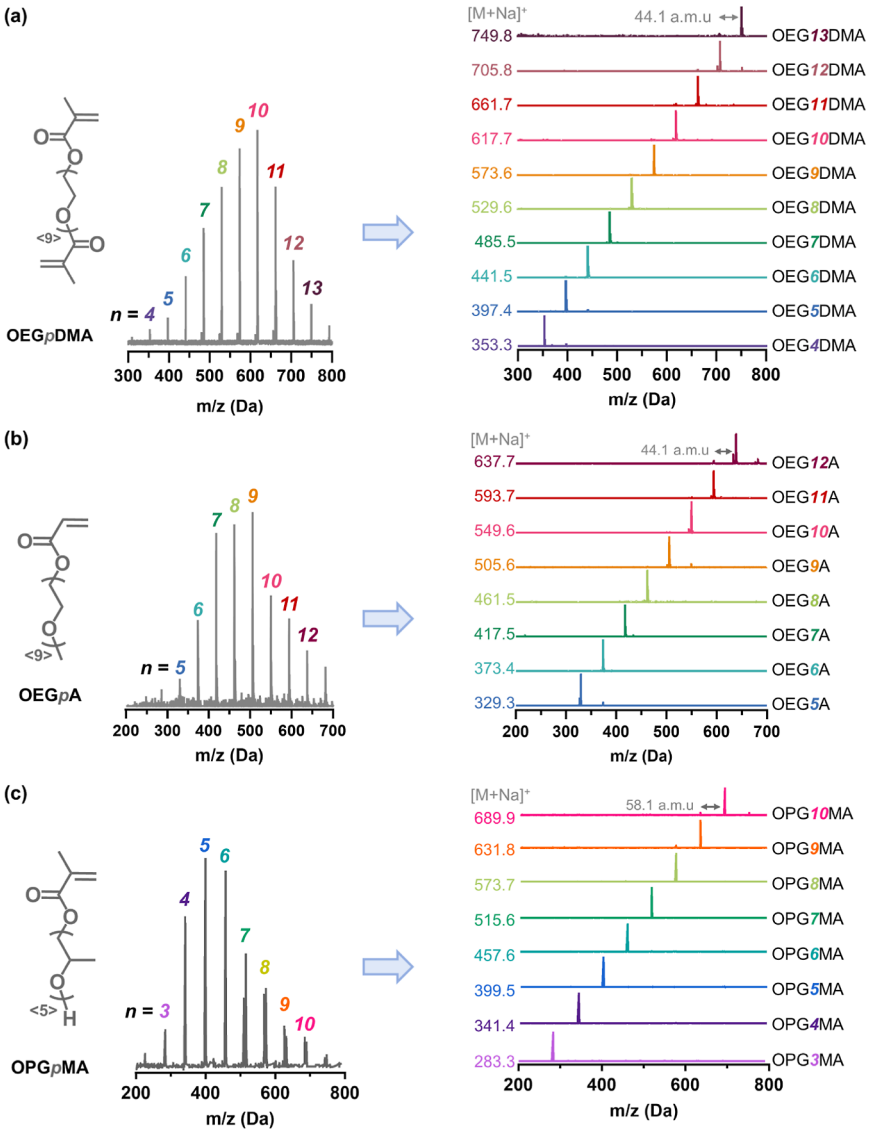

Figure 6. Chemical structures and LC−MS spectra of the (a) OEGDMA, (b) OEGA, and (c) OPGMA macromonomers before and after fractionation using automated chromatography.

The behavior of the graft polymers with intermediate side chain lengths, POEG6MA (n = 6), is distinct in that a two-step change in transmittance is observed during the cooling process, as shown in Figure 5b. This behavior was reproducible, as seen in Figure S11e. The apparent two-step rehydration curve of the POEG6MA solution in the cooling cycle is caused by two different rehydration processes, namely, rehydration of the precipitated chains and rehydration of the polymers within the mesoglobules dispersed in solution. The discrete systems with short side chains (e.g., POEG4MA) tend to precipitate during heating, and the rehydration of the precipitates is the dominant process during cooling. Polymers with longer side chains (e.g., POEGnMA, n = 8−11, Figures 5c,d and S11c,d) are more hydrophilic, with the chains forming stable mesoglobules rather than precipitates; therefore, the rehydration of the mesoglobules is the major process occurring on cooling. POEG6MA shows a balance of hydrophobicity and hydrophilicity with comparable amounts of precipitates and mesoglobules being formed during heating above the LCST. These two components undergo different rehydration processes, leading to the observation of a two-step rehydration process, as shown in Figure 5b. The findings presented above further highlight the potential of automated chromatography for the scalable preparation of building block libraries. These well-defined systems enable a much greater understanding of structure−property relationships.

The fractionation procedure was further extended to three additional commercially available macromonomers, showcasing the versatility of automated chromatography for preparing libraries of discrete polymerizable building blocks. This may be especially important for cross-linkers as the length of the cross-linker defines mesh size in network systems. To illustrate this potential, the commercially available, parent oligo(ethylene glycol) dimethacrylate mixture (OEGpDMA, $\langle M_n \rangle \approx$ 550 g/mol, Figure 6a) was fractionated on scale (8.0 g) to give a library of discrete OEGnDMA macromonomers with precise backbone lengths (Table S3 and Figure S12, 10 species with EG units ranging from 4 to 13, 80% mass recovery, isolated yield ranging from 75 to 1500 mg for each discrete cross-linking species). Similarly, the parent oligo(ethylene glycol) methyl ether acrylate (OEGpA) with an average $\langle M_n \rangle$ of 480 g/mol could be effectively separated into eight discrete species

https://doi.org/10.1021/acs.macromol.4c02533
Macromolecules 2024, 57, 11753−11762

with EG repeating units ranging from 5 to 12 (Table S4, 76% mass recovered from 8.0 g of parent material with isolated yields of the discrete macromonomers ranging from 150 to 1600 mg, Figures 6b and S13). Different side-chain structures could also be separated with this feature being demonstrated using oligo(propylene glycol) methyl ether acrylate (OPG*p*-MA) (average PG units ≈5, $\langle M_n \rangle \approx 375$ g/mol). In this case, five g of OPG*p*MA could be fractionated into discrete OPG*n*MA (n = 3 to 10) with 80% mass recovery and purity comparable to the OEG*n*MA and OEG*n*DMA derivatives described above (Figures 6c, S14 and Table S5). These results demonstrate the versatility of this automated chromatographic strategy for separating commercially available, disperse macromonomers into discrete species in multigram quantities.[30] This allows the preparation of functional grafted polymers and networks with precisely defined side chain or cross-linker structures.[31]

CONCLUSIONS

This report describes a versatile method for preparing grafted polymers with precisely controlled side-chain structures. A series of disperse, commercially available (meth)acrylate macromonomers can be readily fractioned using automated chromatography to produce libraries of the corresponding discrete species in multigram quantities. These discrete monomers and cross-linkers can then be used to prepare grafted polymers and network structures with precisely defined side-chain/cross-linker structures through free radical polymerization. Compared to traditional grafted polymers obtained from disperse monomers, the combined chromatographic fractionation and polymerization strategy enables the exploration with precisely defined materials of the relationship between side-chain structure and physical properties. Specifically, our findings underscore the substantial impact of the side-chain length on thermal and solution properties. This accelerated strategy has the potential to turn dispersed commercial macromonomers into libraries of discrete materials, facilitating the generation of grafted polymers with precisely defined side chains for a range of fundamental studies and high-value applications.

ASSOCIATED CONTENT

Supporting Information

The Supporting Information is available free of charge at https://pubs.acs.org/doi/10.1021/acs.macromol.4c02533.

Materials and synthetic procedures, characterization methods, details of the fractionation process, additional ^{1}H NMR and SEC spectra, kinetics of polymerization, number-average size distributions of polymers, additional plots of transmittance, and DSC thermograms (PDF)

AUTHOR INFORMATION

Corresponding Authors

Andrew K. Whittaker − *Australian Institute for Bioengineering and Nanotechnology, The University of Queensland, Brisbane, Queensland 4072, Australia; Australian Research Council Centre of Excellence for Green Electrochemical Transformation of Carbon Dioxide, The University of Queensland, Brisbane, Queensland 4072, Australia;* orcid.org/0000-0002-1948-8355; Email: a.whittaker@uq.edu.au

Cheng Zhang − *Australian Institute for Bioengineering and Nanotechnology, The University of Queensland, Brisbane, Queensland 4072, Australia; Centre for Advanced Imaging, The University of Queensland, Brisbane, Queensland 4072, Australia;* orcid.org/0000-0002-2722-7497; Email: c.zhang3@uq.edu.au

Authors

Yiqing Wang − *Australian Institute for Bioengineering and Nanotechnology, The University of Queensland, Brisbane, Queensland 4072, Australia; Centre for Advanced Imaging, The University of Queensland, Brisbane, Queensland 4072, Australia*

Xiao Tan − *Australian Institute for Bioengineering and Nanotechnology, The University of Queensland, Brisbane, Queensland 4072, Australia; Centre for Advanced Imaging, The University of Queensland, Brisbane, Queensland 4072, Australia;* orcid.org/0000-0002-9278-6068

Yuhao Zhang − *Australian Institute for Bioengineering and Nanotechnology, The University of Queensland, Brisbane, Queensland 4072, Australia;* orcid.org/0000-0001-5199-172X

David J. T. Hill − *Australian Institute for Bioengineering and Nanotechnology, The University of Queensland, Brisbane, Queensland 4072, Australia; School of Chemistry and Molecular Biosciences, The University of Queensland, St Lucia, Queensland 4072, Australia*

Afang Zhang − *International Joint Laboratory of Biomimetic and Smart Polymers, School of Materials Science and Engineering, Shanghai University, Shanghai 20444, China;* orcid.org/0000-0002-0078-3223

Dehui Kong − *Institute for Molecular Bioscience, The University of Queensland, Brisbane, Queensland 4072, Australia*

Craig J. Hawker − *Materials Research Laboratory, Materials Department, and Department of Chemistry and Biochemistry, University of California Santa Barbara, Santa Barbara, California 93106, United States;* orcid.org/0000-0001-9951-851X

Complete contact information is available at: https://pubs.acs.org/10.1021/acs.macromol.4c02533

Notes

The authors declare no competing financial interest.

ACKNOWLEDGMENTS

The authors acknowledge the Australian Research Council (DP210101496 and LP220100036) and The University of Queensland Knowledge Exchange & Translation Grant for funding of this research. C.Z. acknowledges the National Health and Medical Research Council for his CJ Martin Fellowship (APP1157440) and the Australian Research Council for his Discovery Early Career Researcher Award fellowship (DE230101105). C.J.H. acknowledges support from the NSF BioPACIFIC Materials Innovation Platform of the National Science Foundation under award no. DMR-1933487. This work used the Queensland node of the NCRIS-enabled Australian National Fabrication Facility (ANFF).

REFERENCES

(1) Takizawa, K.; Tang, C.; Hawker, C. J. Molecularly defined caprolactone oligomers and polymers: synthesis and characterization. *J. Am. Chem. Soc.* **2008**, *130* (5), 1718−1726.

(2) Hawker, C. J.; Malmström, E. E.; Frank, C. W.; Kampf, J. P. Exact linear analogs of dendritic polyether macromolecules: design, synthesis, and unique properties. *J. Am. Chem. Soc.* **1997**, *119* (41), 9903−9904.
(3) van Genabeek, B.; Lamers, B. A.; Hawker, C. J.; Meijer, E.; Gutekunst, W. R.; Schmidt, B. V. Properties and applications of precision oligomer materials; where organic and polymer chemistry join forces. *J. Polym. Sci.* **2021**, *59* (5), 373−403.
(4) Zhang, C.; Bates, M. W.; Geng, Z.; Levi, A. E.; Vigil, D.; Barbon, S. M.; Loman, T.; Delaney, K. T.; Fredrickson, G. H.; Bates, C. M.; Whittaker, A. K.; Hawker, C. J. Rapid generation of block copolymer libraries using automated chromatographic separation. *J. Am. Chem. Soc.* **2020**, *142* (21), 9843−9849.
(5) Ogbonna, N. D.; Dearman, M.; Cho, C. T.; Bharti, B.; Peters, A. J.; Lawrence, J. Topologically precise and discrete bottlebrush polymers: synthesis, characterization, and Structure−Property relationships. *JACS Au* **2022**, *2* (4), 898−905.
(6) Lawrence, J.; Lee, S.-H.; Abdilla, A.; Nothling, M. D.; Ren, J. M.; Knight, A. S.; Fleischmann, C.; Li, Y.; Abrams, A. S.; Schmidt, B. V.; Hawker, M. C.; Connal, L. A.; McGrath, A. J.; Clark, P. G.; Gutekunst, W. R.; Hawker, C. J. A versatile and scalable strategy to discrete oligomers. *J. Am. Chem. Soc.* **2016**, *138* (19), 6306−6310.
(7) Lawrence, J.; Goto, E.; Ren, J. M.; McDearmon, B.; Kim, D. S.; Ochiai, Y.; Clark, P. G.; Laitar, D.; Higashihara, T.; Hawker, C. J. A versatile and efficient strategy to discrete conjugated oligomers. *J. Am. Chem. Soc.* **2017**, *139* (39), 13735−13739.
(8) Ren, J. M.; Lawrence, J.; Knight, A. S.; Abdilla, A.; Zerdan, R. B.; Levi, A. E.; Oschmann, B.; Gutekunst, W. R.; Lee, S. H.; Li, Y.; McGrath, A. J.; Bates, C. M.; Qiao, G. G.; Hawker, C. J. Controlled formation and binding selectivity of discrete oligo (methyl methacrylate) stereocomplexes. *J. Am. Chem. Soc.* **2018**, *140* (5), 1945−1951.
(9) Zhang, C.; Kim, D. S.; Lawrence, J.; Hawker, C. J.; Whittaker, A. K. Elucidating the impact of molecular structure on the 19F NMR dynamics and mri performance of fluorinated oligomers. *ACS Macro Lett.* **2018**, *7* (8), 921−926.
(10) Murphy, E. A.; Zhang, C.; Bates, C. M.; Hawker, C. J. Chromatographic separation: a versatile strategy to prepare discrete and well-defined polymer libraries. *Acc. Chem. Res.* **2024**, *57* (8), 1202−1213.
(11) Chen, J.; Rizvi, A.; Patterson, J. P.; Hawker, C. J. Discrete libraries of amphiphilic poly (ethylene glycol) graft copolymers: synthesis, assembly, and bioactivity. *J. Am. Chem. Soc.* **2022**, *144* (42), 19466−19474.
(12) Romio, M.; Grob, B.; Trachsel, L.; Mattarei, A.; Morgese, G.; Ramakrishna, S. N.; Niccolai, F.; Guazzelli, E.; Paradisi, C.; Martinelli, E.; et al. Dispersity within brushes plays a major role in determining their interfacial properties: the case of oligoxazoline-based graft polymers. *J. Am. Chem. Soc.* **2021**, *143* (45), 19067−19077.
(13) Dearman, M.; Ogbonna, N. D.; Amofa, C. A.; Peters, A. J.; Lawrence, J. Versatile strategies to tailor the glass transition temperatures of bottlebrush polymers. *Polym. Chem.* **2022**, *13* (34), 4901−4907.
(14) Lutz, J. F. Polymerization of oligo (ethylene glycol)(meth) acrylates: toward new generations of smart biocompatible materials. *J. Polym. Sci., Part A: Polym. Chem.* **2008**, *46* (11), 3459−3470.
(15) Yang, J.; Gitlin, I.; Krishnamurthy, V. M.; Vazquez, J. A.; Costello, C. E.; Whitesides, G. M. Synthesis of monodisperse polymers from proteins. *J. Am. Chem. Soc.* **2003**, *125* (41), 12392−12393.
(16) Deng, Z.; Shi, Q.; Tan, J.; Hu, J.; Liu, S. Sequence-defined synthetic polymers for new-generation functional biomaterials. *ACS Mater. Lett.* **2021**, *3* (9), 1339−1356.
(17) Meier, M. A. R.; Barner-Kowollik, C. A new class of materials: sequence-defined macromolecules and their emerging applications. *Adv. Mater.* **2019**, *31* (26), 1806027.
(18) Oschmann, B.; Lawrence, J.; Schulze, M. W.; Ren, J. M.; Anastasaki, A.; Luo, Y.; Nothling, M. D.; Pester, C. W.; Delaney, K. T.; Connal, L. A.; McGrath, A. J.; Clark, P. G.; Bates, C. M.; Hawker, C. J. Effects of tailored dispersity on the self-assembly of dimethylsiloxane-methyl methacrylate block co-oligomers. *ACS Macro Lett.* **2017**, *6* (7), 668−673.
(19) Vleugels, M. E. J.; de Zwart, M. E.; Magana, J. R.; Lamers, B. A. G.; Voets, I. K.; Meijer, E. W.; Petkau-Milroy, K.; Palmans, A. R. A. Effects of crystallinity and dispersity on the self-assembly behavior of block co-oligomers in water. *Polym. Chem.* **2020**, *11* (45), 7170−7177.
(20) Zhang, C.; Moonshi, S. S.; Han, Y.; Puttick, S.; Peng, H.; Magoling, B. J. A.; Reid, J. C.; Bernardi, S.; Searles, D. J.; Král, P.; et al. PFPE-based polymeric 19F MRI agents: a new class of contrast agents with outstanding sensitivity. *Macromolecules* **2017**, *50* (15), 5953−5963.
(21) Tan, X.; Zhong, J. X.; Fu, C. K.; Dang, H.; Han, Y. X.; Král, P.; Guo, J. H.; Yuan, Z. G.; Peng, H.; Zhang, C.; Whittaker, A. K. Amphiphilic perfluoropolyether copolymers for the effective removal of polyfluoroalkyl substances from aqueous environments. *Macromolecules* **2021**, *54* (7), 3447−3457.
(22) Tsukahara, Y.; Namba, S.-i.; Iwasa, J.; Nakano, Y.; Kaeriyama, K.; Takahashi, M. Bulk properties of poly(macromonomer)s of increased backbone and branch lengths. *Macromolecules* **2001**, *34* (8), 2624−2629.
(23) Ishino, K.; Shingai, H.; Hikita, Y.; Yoshikawa, I.; Houjou, H.; Iwase, K. Cold crystallization and the molecular structure of imidazolium-based ionic liquid crystals with ap-nitroazobenzene moiety. *ACS Omega* **2021**, *6* (48), 32869−32878.
(24) Honda, A.; Kakihara, S.; Kawai, M.; Takahashi, T.; Miyamura, K. Cold crystallization and polymorphism triggered by the mobility of the phenyl group in alkyl azo dye molecules. *Cryst. Growth Des.* **2021**, *21* (11), 6223−6229.
(25) Park, W.; Park, S. J.; Cho, S.; Shin, H.; Jung, Y. S.; Lee, B.; Na, K.; Kim, D. H. Intermolecular structural change for thermoswitchable polymeric photosensitizer. *J. Am. Chem. Soc.* **2016**, *138* (34), 10734−10737.
(26) Kim, Y. H.; Kwon, I. C.; Bae, Y. H.; Kim, S. W. Saccharide effect on the lower critical solution temperature of thermosensitive polymers. *Macromolecules* **1995**, *28* (4), 939−944.
(27) Zhang, C.; Peng, H.; Whittaker, A. K. NMR investigation of effect of dissolved salts on the thermoresponsive behavior of oligo (ethylene glycol)-methacrylate-based polymers. *J. Polym. Sci., Part A: Polym. Chem.* **2014**, *52* (16), 2375−2385.
(28) Lutz, J.-F.; Weichenhan, K.; Akdemir, Ö.; Hoth, A. About the phase transitions in aqueous solutions of thermoresponsive copolymers and hydrogels based on 2-(2-methoxyethoxy) ethyl methacrylate and oligo (ethylene glycol) methacrylate. *Macromolecules* **2007**, *40* (7), 2503−2508.
(29) Lutz, J.-F.; Akdemir, Ö.; Hoth, A. Point by point comparison of two thermosensitive polymers exhibiting a similar LCST: is the age of poly (NIPAM) over? *J. Am. Chem. Soc.* **2006**, *128* (40), 13046−13047.
(30) Shu, Y.; Pang, H.; Wu, Y.; Wang, Y.; Huang, G.; Zhang, C.; Han, F. Y. Rapid generation of well-defined biodegradable poly-(lactide-co-glycolide) libraries through chromatographic separation. *J. Polym. Sci.* **2024**, *62* (17), 4091−4100.
(31) Yang, Z.; Zhu, Y.; Tan, X.; Gunjal, S. J. J.; Dewapriya, P.; Wang, Y.; Xin, R.; Fu, C.; Liu, K.; Macintosh, K.; et al. Fluoropolymer sorbent for efficient and selective capturing of per- and polyfluorinated compounds. *Nat. Commun.* **2024**, *15* (1), 8269.

https://doi.org/10.1021/acs.macromol.4c02533
Macromolecules 2024, 57, 11753−11762